

MANEUVER LOADS BRANCH COPY

1221

NATIONAL ADVISORY COMMITTEE FOR AERONAUTICS

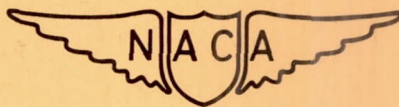
TECHNICAL NOTE

No. 1221

EFFECT OF EXHAUST PRESSURE ON THE COOLING
CHARACTERISTICS OF AN AIR-COOLED ENGINE

By Michael F. Valerino, Samuel J. Kaufman
and Richard F. Hughes

Aircraft Engine Research Laboratory
Cleveland, Ohio



Washington
March 1947

NATIONAL ADVISORY COMMITTEE FOR AERONAUTICS

TECHNICAL NOTE NO. 1221

EFFECT OF EXHAUST PRESSURE ON THE COOLING
CHARACTERISTICS OF AN AIR-COOLED ENGINE

By Michael F. Valerino, Samuel J. Kaufman
and Richard F. Hughes

SUMMARY

The results of a cooling investigation conducted on an 18-cylinder, radial, air-cooled engine installed on a dynamometer test stand were analyzed to determine the effect of exhaust pressure on the engine-cooling characteristics. The tests covered a wide range of engine operating conditions including exhaust pressures from 7 to 65 inches of mercury absolute.

The effect of exhaust pressure on engine cooling was incorporated in the NACA engine-cooling correlation method as a variation in engine mean effective gas temperature with exhaust pressure. The effect of exhaust pressure on average cylinder-head temperature can be predicted from the correlation within about 6° F for exhaust pressures ranging from approximately 10 to 50 inches of mercury absolute.

Calculations based on the test results indicate that for operation at constant power, equal to the engine normal rated power, at a fuel-air ratio of 0.085 the head temperature increases 39° F when the exhaust pressure is increased from 10 to 50 inches of mercury absolute. For operation at constant inlet-manifold pressure, however, the effect of mean effective gas temperature is for the most part counteracted by the effect of reduced power obtained with increase in exhaust pressure; for example, for a constant inlet-manifold pressure of 30 inches of mercury absolute at a fuel-air ratio of 0.085 the head-temperature increase is only 7° F for an increase in exhaust pressure from 10 to 50 inches of mercury absolute.

The effect of exhaust pressure on engine cooling is greater at the lean than the rich mixtures.

INTRODUCTION

The effect of exhaust pressure on the performance and cooling characteristics of aircraft engines is of importance because of the

wide altitude range of general airplane operation and the current widespread interest in engine-turbine combinations. Little information is available concerning the exhaust-pressure variable, particularly regarding its relation to engine cooling.

The effect of exhaust pressure on engine cooling was recognized by Pinkel in 1938 and included as a possible factor in the cooling-correlation method developed in reference 1 but no test data were presented. The results of the limited investigation of reference 2 indicated that the effect of exhaust pressure on engine cooling is small; however, because so little data were obtained in these tests, the results are inconclusive. Although numerous engine-cooling investigations have been conducted subsequent to the reported results of references 1 and 2, the tests have been at or near sea-level exhaust pressures and permitted no systematic study of the exhaust-pressure variable as affecting engine cooling.

An investigation was conducted at the NACA Cleveland laboratory to determine the effect of exhaust pressure on the performance of an 18-cylinder, radial, air-cooled engine installed on a dynamometer test stand. Data for relating the engine-cooling characteristics with the exhaust-pressure variable were also obtained. The results of the analyses of the engine-performance data obtained in these tests are presented in reference 3. The cooling data obtained are analyzed herein by the NACA engine-cooling correlation method to show the effect of exhaust pressure on engine cooling.

The test conditions ranged as follows: inlet-manifold pressure, 30 to 45 inches of mercury absolute; engine speed, 1200 to 2400 rpm; fuel-air ratio, 0.069 to 0.120; exhaust pressure, 7 to 65 inches of mercury absolute. Low-blower operation was used in most of the runs, but a few runs were made in high-blower operation.

INSTALLATION AND INSTRUMENTATION

Equipment

The investigation was conducted on an R-2800-5, series A, multi-cylinder engine equipped with a two-speed single-stage engine supercharger, which has an impeller diameter of 11 inches and a gear ratio of 7.6:1 in low-blower operation and 9.45:1 in high-blower operation. An injection-type carburetor, slightly modified to permit direct control of the engine fuel flow, was used in the runs. The valve overlap for the engine is 40° , the bore and stroke $5\frac{3}{4}$ inches by 6 inches, the compression ratio 6.65, and the spark setting 25° B.T.C. The engine is rated as follows:

Take-off	1850 bhp at 2600 rpm
Maximum continuous operation:	
Low blower	1500 bhp at 2400 rpm
High blower	1450 bhp at 2400 rpm

The complete installation is adequately described in reference 3; for convenience, however, a detailed description of the parts of the installation that are closely associated with the control and measurement of the basic engine-cooling variables is presented. A photograph and sketch of the installation is presented in figures 1 and 2 showing the engine rigidly mounted for connection through an extension shaft to a 2000-horsepower eddy-current dynamometer, the cooling-air box and engine cowling, and the elbow section of the exhaust-gas ducting.

Cooling air from the laboratory supply system was delivered to the top of the cooling-air box from where it flowed through a streamlined nozzle section to the front face of the engine. The air box functioned as a large air reservoir for providing a uniform cooling-air distribution over the face of the engine. The engine was cowed with a cylindrical duct as shown in figure 1. The cooling air after flowing across the engine discharged directly into the room.

The exhaust-gas collector ring, which was the type used in the turbosupercharger installations on the P-47 airplane, consists of two half sections, one for each side of the engine. The two sections were joined at the bottom by a Y-shaped duct that was directly connected to the laboratory altitude-exhaust system. The exhaust pressure was measured by a static wall tap located at the cross section where the Y-shaped duct was bolted to the exhaust-duct elbow.

The carburetor-air duct (figs. 1 and 2), which supplied charge air to the engine, incorporated a long straight constant-area section of piping so installed directly upstream of the carburetor that substantially uniform flow conditions prevailed at the carburetor top deck. The engine throttle was kept wide open and the charge-air flow was regulated by a butterfly valve located near the duct entrance. Charge-air-flow measurements were made with a thin-plate orifice designed and installed in the duct system in accordance with A.S.M.E. specifications. The fuel flow was measured with a calibrated rotameter.

Temperature Measurements

Cylinder temperatures were measured with iron-constantan thermocouples at the following locations on each cylinder: rear spark-plug gasket, rear center of barrel, and embedded deeply in rear spark-plug

boss. The gasket thermocouples were made by silver-soldering the thermocouple wires into a small hole drilled into the tab to the outer edge of the copper spark-plug gasket. The barrel thermocouples were peened into the aluminum barrel muff's at the rear between the two middle barrel fins. As sketched in figure 3, the boss thermocouples were inserted in brass plugs and embedded 30 percent of the cylinder-wall thickness at a point $45/64$ inch from the spark-plug axis and 45° from the bottom of the spark-plug boss toward the exhaust port.

Three thermocouples were located in the cooling-air stream directly in front of the engine 120° apart; six thermocouples connected in parallel were located in the charge-air stream at the carburetor top deck. All temperatures were read on a self-balancing potentiometer.

Cooling-Air Pressure Measurements

Because of the unusually uniform cooling-air pressure patterns existing ahead of and behind the engine, a relatively small number of tubes were used to measure the cooling-air pressure drop. The cooling-air total pressure was measured ahead of the engine with six shrouded total-head tubes, two tubes mounted on each of three rakes installed directly in front of the engine 120° apart. The outer tubes of each rake were at the same radial distance as the middle circumferential head fin; the inner tubes were at the same radial distance as the middle barrel fin.

The cooling-air static pressure behind the cylinder heads was measured with open-end tubes placed in the baffle curl of the nine rear-row cylinders at the same radius as the total-head tubes. These static tubes were installed in such a position that they received little if any velocity pressure. The static pressure behind the barrels was measured by three closed-end static tubes, one on each of three rakes behind three rear-row cylinder barrels 120° apart at the same radial distance as the barrel total-head tubes.

PROCEDURE

Two general groups of runs were made: (1) runs in which the cooling characteristics of the engine were established for the sea-level exhaust-pressure condition, and (2) runs in which the cooling characteristics of the engine were obtained with variable exhaust pressure.

The sea-level exhaust pressure data were used to determine the separate effects of charge-air flow, fuel-air ratio, and cooling-air pressure drop on engine cooling. The effect of exhaust pressure was determined from the data obtained in a comprehensive series of tests conducted at variable exhaust pressures for a wide range of inlet-manifold pressures, engine speeds, and fuel-air ratios. A complete list of the operating conditions is given in table I.

The procedure in the second group of runs was to maintain inlet-manifold pressure, engine speed, and fuel-air ratio at definite specified values while the exhaust pressure was varied in increments from approximately 7 inches of mercury absolute to 20 inches of mercury above the inlet-manifold pressure. Sufficient time was allowed at each value of exhaust pressure for the cylinder temperature to stabilize. For each series of runs at variable exhaust pressure, the cooling-air pressure drop was adjusted to a value that kept the maximum rear-spark-plug-gasket temperature at a value between 375° and 425° F when the exhaust pressure was approximately 28 inches of mercury absolute; the cooling-air pressure drop was then held constant during the series while the exhaust pressure was varied.

CORRELATION METHOD

One form of the equation developed in reference 1 for relating the wall temperatures of air-cooled engines with the engine operating and cooling-air conditions is

$$\frac{T_h - T_a}{T_g - T_h} = K \frac{W_c^n}{(\sigma \Delta p)^m} \quad (1)$$

where

- T_h cylinder-head temperature, °F
- T_a cooling-air temperature ahead of engine, °F
- T_g mean effective gas temperature, °F
- W_c engine charge-air flow, pounds per second
- σ density of cooling air ahead of engine relative to standard sea-level density of 0.0765 pound per cubic foot
- Δp cooling-air pressure drop across engine, inches of water
- K, m, n constants derived from proper cooling data

Additional symbols are defined in appendix A.

The equation for correlating the cylinder-barrel temperature T_b is similar to equation (1) for the cylinder heads. The procedure involved in using equation (1) to correlate the engine-cooling data is explained in references 4 and 5 and briefly reviewed in appendix B.

The primary engine operating conditions (engine speed, inlet-manifold pressure and temperature, fuel-air ratio, exhaust pressure, and spark advance) are not specifically indicated in equation (1). The effects of engine speed and inlet-manifold pressure on engine cooling are accounted for in equation (1) through their influence on W_c ; the effects of fuel-air ratio, inlet-manifold temperature, and spark advance are included primarily through their influence on T_g . The effect of exhaust pressure on engine cooling may be included in equation (1) through its effect on both W_c and T_g , as is described in the following paragraph.

Two distinct factors affecting engine cooling are involved when the exhaust pressure is varied. The first factor is associated with the change of engine charge-air flow and its effect on cooling is directly included in the correlation through the use of W_c in equation (1). The second factor is associated with the change in exhaust-gas residuals, which affects both the temperature and composition of the cylinder charge; its effect is included in the correlation as a variation of T_g . Theoretically, the effect of residuals on T_g is a function of the ratio of the exhaust pressure to the inlet-manifold pressure rather than of exhaust or manifold pressure separately. In past correlations for cooling data obtained at sea-level exhaust-pressure conditions, the effect of manifold pressure was separated however, and included with the effect of charge-air flow in equation (1). This procedure was adopted primarily in the interest of simplicity. In order to be consistent with previous cooling correlations, this same simplification will be adhered to in this analysis. The effect of exhaust pressure on T_g is therefore treated as an isolated effect independent of inlet-manifold pressure. The scatter of the data indicates the accuracy of the simplification.

Details of the procedure for analysis of the data are as follows:

Cylinder temperatures and cooling-air temperature and pressures. -

The value of cylinder-head temperature T_h in cooling-correlation equation (1) is taken as the average of the temperature indications of the thermocouples deeply embedded in the rear spark-plug bosses; the cylinder-barrel temperature T_b is taken as the average of the temperature indications of the thermocouples peened in the rear middle of the barrels. The average of the readings of the three thermocouples in the cooling-air stream is taken as the cooling-air temperature ahead of the engine.

The cooling-air pressure drop $\sigma\Delta p$ across the cylinder heads is taken as the difference between the average total pressure ahead of and the average static pressure behind the cylinder heads corrected to sea-level density conditions. The cooling-air pressure drop across the cylinder barrels is obtained in the same manner using the pressures ahead of and behind the barrels.

Correlation of sea-level exhaust-pressure cooling data. - The cooling data obtained in the sea-level exhaust-pressure runs are reduced to determine the variation of $T_{g,80}$ (mean effective gas temperature corrected to 80° F dry inlet-manifold temperature) with fuel-air ratio and the constant K and exponents n and m in the head and barrel correlation equations. The method used in this cooling-data correlation is explained in references 4 and 5 and briefly outlined in appendix B.

Determination of exhaust-pressure effect on T_g . - Inasmuch as in each variable exhaust-pressure series of runs the inlet-manifold pressure, fuel-air ratio, engine speed, and cooling-air pressure drop were kept constant, the measured variation in engine cooling represents the net result of two principal factors: (1) the change in charge-air flow with exhaust pressure; and (2) the change in mean effective gas temperature with exhaust pressure. The effect of the change in charge-air flow on engine cooling is calculated from the basic correlation equation established in appendix B for the cylinder heads and barrels from the sea-level exhaust-pressure data. The change in engine cooling caused by the change in mean effective gas temperature during each series of runs is thus isolated, which permits ready calculation of the mean effective gas temperature variation with exhaust pressure. In detail, the foregoing procedure is reduced to the following simple steps:

(1) The head and barrel values of $\frac{T_h - T_a}{T_g - T_h} / W_c^n$ and $\frac{T_b - T_a}{T_g - T_b} / W_c^n$ are calculated for the sea-level exhaust-pressure run in each series. The T_g values applicable in these calculations were obtained through the use of the $T_{g,80}$ relation with fuel-air ratio as established for sea-level exhaust pressure. The conversion between T_g and $T_{g,80}$ is described in appendix B.

(2) Inasmuch as the values of $\frac{T_h - T_a}{T_g - T_h} / W_c^n$ and $\frac{T_b - T_a}{T_g - T_b} / W_c^n$ are constant in each series at variable exhaust pressure (because of constant $\sigma\Delta p$), solution for T_g and thus $T_{g,80}$ is made from these constant calculated values and the measured test values in each run of the test series of T_h , T_b , T_a , and W_c .

(3) Two refinements are included in the calculations previously outlined. The first refinement is a slight correction for the small unavoidable variations in cooling-air pressure drop obtained in each run series. A second small correction was made because the sea-level exhaust-pressure run in each series was actually made at an exhaust-pressure value ranging from 29 to 32 inches of mercury absolute.

Charge-air flow. - The method for estimating the charge-air flow corresponding to the other engine operating conditions (brake horsepower, speed, fuel-air ratio, and exhaust- and inlet-manifold pressures), as required prior to application of the cooling-correlation results, is presented in appendix C. The applicability of this method is checked in detail in reference 3 from a consideration of all the performance data obtained in the runs. Reference 3 shows that, except for engine operation at a low exhaust pressure of 10 inches of mercury absolute for engine speeds of 1200 and 1400 rpm, estimations of charge-air flow within ± 2.5 percent can be made by this method.

The variation of brake horsepower with exhaust pressure for constant inlet-manifold pressure and other constant engine operating conditions, which is of importance for use with the aforementioned method in determining the variation in charge-air flow with exhaust pressure, is discussed in appendix C.

RESULTS AND DISCUSSION

The results of the investigation indicate that the effect of exhaust pressure on engine cooling is important enough to require consideration in engine-cooling correlations and predictions. The details of the results are presented.

Correlation equation. - The cooling characteristics of the cylinder heads and barrels, as determined from the cooling data (appendix B), are conveniently described in figure 4 by a plot on log-log coordinates of $\frac{T_h - T_a}{T_g - T_h} / W_c^{0.62}$ and $\frac{T_b - T_a}{T_g - T_b} / W_c^{0.57}$ against the appropriate $\sigma \Delta p$ values. The resulting correlation equations may be expressed from figure 4 as

$$\frac{T_h - T_a}{T_g - T_h} = 0.44 \frac{W_c^{0.62}}{(\sigma \Delta p)^{0.30}}, \text{ cylinder heads} \quad (2)$$

and

$$\frac{T_b - T_a}{T_g - T_b} = 0.68 \frac{W_c^{0.57}}{(\sigma \Delta p)^{0.39}}, \text{ cylinder barrels} \quad (3)$$

Variation of $T_{g,80}$ with exhaust pressure. - The results of the effect of exhaust pressure on engine cooling are presented in figure 5 where the mean effective gas temperature $T_{g,80}$ for the heads and barrels is plotted for each datum point against the corresponding exhaust-pressure value. A curve is drawn through the plotted points for each of the four fuel-air ratios used. The curves are dashed for exhaust pressures above approximately 50 inches of mercury absolute to indicate extrapolation as based on the trends of the curves and on the limited data for the inlet-manifold pressures of 40 and 45 inches of mercury absolute. (Trend exists with inlet-manifold pressure, as subsequently discussed.)

Except for the exhaust pressures of 7 to 10 inches of mercury absolute and above approximately 50 inches of mercury absolute, the average deviation of the data from the appropriate curve is about $\pm 20^\circ$ F for the heads and $\pm 15^\circ$ F for the barrels. These scatters are roughly equivalent to $\pm 6^\circ$ F and $\pm 5^\circ$ F deviations in average rear-spark-plug-boss and rear-middle-barrel temperatures, respectively.

Close examination of the data points in figure 5 reveals that the scatter of data does not occur at random but that a trend exists with inlet-manifold pressure, particularly in the range of exhaust pressures above 50 inches of mercury absolute. The presence of this trend indicates that the effect of inlet-manifold pressure is not completely accounted for by equation (1).

In addition, at the low exhaust pressures of about 7 to 10 inches of mercury absolute a trend with engine speed appears. In order to bring out this trend in the data, a cross plot of the $T_{g,80}$ values for the cylinder heads obtained at an exhaust pressure of approximately 8 inches of mercury absolute and at a fuel-air ratio of 0.085 is presented in figure 6. The cross plot shows an appreciable increase in $T_{g,80}$ with engine speed and in addition, a slight increase with manifold pressure at this exhaust pressure.

A possible explanation for this speed effect obtained at very low exhaust pressures may be that sufficient flow of fresh charge air through the cylinder and out of the exhaust port takes place at the low exhaust pressures to affect engine cooling and that the percentage of blow-through depends on the engine speed. An indication of the blow-through and its dependence on engine speed is shown in figure 7 where the ratio of the specific indicated air consumption obtained at a given inlet-manifold pressure p_m for various exhaust pressures p_e to that obtained at $p_e/p_m = 1$ (for which no blow-through would be expected) is plotted against exhaust pressure for

the various engine speeds and for constant values of fuel-air ratio and manifold pressure. The curves show that when the exhaust pressure is reduced from 16 to 8 inches of mercury absolute a sharp increase in specific indicated air consumption occurs, the magnitude of which increases with reduction in engine speed. This blow-through may be the result of the intake-valve motion characteristics at the high differentials between inlet-manifold and exhaust pressures, inasmuch as an investigation on a later model engine with the same valve overlap but stronger intake-valve springs did not result in blow-through. These results show that the speed effect on cooling obtained at very low exhaust pressures is associated and consistent with the change in percentage blow-through obtained with change in engine speed. It may be expected that this speed effect would be considerably reduced for engines with heavier intake-valve springs and attendant lesser blow-through.

As a result of the aforementioned inlet-manifold pressure and speed trends, the accuracy of prediction of head temperature from the correlation is only about 15° to 20° F for the exhaust pressures of 7 to 10 inches of mercury absolute and above 50 inches of mercury absolute. For exhaust pressures above approximately 10 and below approximately 50 inches of mercury absolute, however, predictions of the variation of head temperature with exhaust pressure can be made within about 6° F. Thus the simplification of handling T_g as a function of exhaust pressure rather than of the ratio of exhaust to inlet-manifold pressure seems to be satisfactory within exhaust-pressure limits that adequately cover the practical limits of current engine operation.

Final $T_{g,80}$ relations. - A cross plot of the curves of figure 5 shows the variation of mean effective gas temperature $T_{g,80}$ with fuel-air ratio at various exhaust pressures (fig. 8). Because of the relatively poor $T_{g,80}$ correlation obtained at exhaust pressure above 50 inches of mercury absolute, $T_{g,80}$ curves are not presented above this exhaust-pressure value. Although, as a result of the previously discussed speed effect, the $T_{g,80}$ variation cannot be accurately represented for exhaust pressures of approximately 10 inches of mercury absolute, the $T_{g,80}$ curves are also given for the exhaust pressure of 10 inches of mercury absolute for use in making approximate solutions. Figure 8 shows that the effect of exhaust pressure on mean effective gas temperature is greater at the lean than at the rich mixtures.

Importance of exhaust-pressure effect. - In order to illustrate the necessity of accounting for the effect of exhaust pressure in engine-cooling correlations, all the cooling data obtained in the

variable exhaust-pressure test series at an absolute manifold pressure of 34 inches of mercury are correlated first by neglecting the exhaust-pressure effect and then by correcting for the exhaust-pressure variations through the use of the $T_{g,80}$ curves of figure 8. The correlation results plotted in figure 9 show a relatively large spread of data when the exhaust-pressure effect is not included and indicate an exhaust-pressure trend large enough to require consideration.

Figures 10 to 12 are presented for typical sets of engine operating and cooling-air conditions in order to illustrate the effect of exhaust pressure on engine cooling. Figure 10 shows that, for the assumed set of conditions, when the exhaust pressure is changed from 30 inches of mercury absolute and the inlet-manifold pressure is adjusted to maintain constant charge-air flow (approximately constant power equal to normal rated power) the following changes in head and barrel temperatures are obtained:

Exhaust pressure (in. Hg absolute)	Change in head temperature from the value at exhaust pressure of 30 in. Hg absolute (°F)			Change in barrel temperature from the value at exhaust pressure of 30 in. Hg absolute (°F)		
	Fuel-air ratio					
	0.069	0.085	0.100	0.069	0.085	0.100
10	-22	-13	-7	-9	-5	-1
20	-14	-8	-5	-5	-3	-1
30	0	0	0	0	0	0
40	19	12	9	5	4	1
50	43	26	18	14	10	5

When the inlet-manifold pressure is held constant during the change in exhaust pressure, in which case a significant variation in engine-power output with exhaust pressure is also obtained, however, the head and barrel temperatures vary in the manner shown in figure 11 and as shown in the following table:

Exhaust pressure (in. Hg absolute)	Change in head temperature from the value at exhaust pressure of 30 in. Hg absolute (°F)			Change in barrel temperature from the value at exhaust pressure of 30 in. Hg absolute (°F)		
	Fuel-air ratio					
	0.069	0.085	0.100	0.069	0.085	0.100
10	-12	-3	1	-3	1	5
20	-7	-2	0	-1	1	3
30	0	0	0	0	0	0
40	9	4	0	0	-1	-3
50	17	4	-4	1	-3	-7

The head- and barrel-temperature variations indicated in figure 10 for constant charge-air flow are the result solely of the variation in mean effective gas temperature with exhaust pressure; whereas in figure 11, which is presented for constant inlet-manifold pressure, an additional effect is introduced due to the variation in charge-air flow with exhaust pressure. Figures 10 and 11 show that for operation at constant inlet-manifold pressure the effect on engine cooling of the variation in mean effective gas temperature with exhaust pressure is counteracted to a large extent by the effect of the accompanying change in charge-air flow with exhaust pressure. The variation of charge-air flow (and brake horsepower) with exhaust pressure for the assumed set of engine conditions is indicated in figure 11. From this figure it can be seen that for operation at constant inlet-manifold pressure a change in exhaust pressure from 30 to either 10 or 50 inches of mercury absolute does not give more than about 5° F change in head and barrel temperatures at fuel-air ratios of 0.085 and 0.100 for the heads and at fuel-air ratios of 0.069, 0.085, and 0.100 for the barrels. At a fuel-air ratio of 0.069, the equivalent change in head temperature is indicated as about 15° F. Although figure 10 is presented for an assumed set of engine and cooling-air conditions, the same general results are indicated for other normal engine conditions by the test data and by the correlation results.

The variation with exhaust pressure of the cooling-air pressure drop required to maintain a constant average head temperature of 400° F and a constant average barrel temperature of 300° F is shown in figure 12 for the case in which the charge-air flow and other engine and cooling conditions were maintained constant throughout the exhaust-pressure range. The results of figure 12 are summarized in the following table:

Exhaust pressure (in. Hg absolute)	Change in cooling-air pressure drop from that required at an exhaust pressure of 30 in. Hg absolute to maintain constant head temperature of 400° F (in. water)			Change in cooling-air pressure drop from that required at an exhaust pressure of 30 in. Hg absolute to maintain constant barrel temperature of 300° F (in. water)		
	Fuel-air ratio					
	0.069	0.085	0.100	0.069	0.085	0.100
10	-1.9	-1.0	-0.4	-0.4	-0.1	0
20	-1.2	-.6	-.3	-.2	-.1	0
30	0	0	0	0	0	0
40	2.0	1.0	.4	.3	.2	.1
50	4.9	2.3	1.0	.8	.5	.2

SUMMARY OF RESULTS

The results of a cooling investigation conducted on an 18-cylinder, radial, air-cooled engine installed on a dynamometer test stand show that:

1. The effect of exhaust pressure on engine cooling was important enough to require consideration in engine-cooling correlations and predictions.

2. For the range of inlet-manifold pressures used in the investigation and for exhaust pressures between approximately 10 and 50 inches of mercury absolute, the exhaust-pressure effect on engine cooling could be satisfactorily represented (permitted predictions of head temperature within about 6° F) in the NACA cooling-correlation method as the variation of mean effective gas temperature with exhaust pressure.

3. Above an exhaust pressure of 50 inches of mercury absolute, an effect associated with inlet-manifold pressure became important and caused discrepancies in the relation between mean effective gas temperature and exhaust pressure. For exhaust pressures below approximately 10 inches of mercury absolute an effect associated with engine speed was obtained for this engine (having blow-through of charge air through cylinder) causing excessive scatter of data. As a result of the inlet-manifold and speed effects, predictions of the effect of exhaust pressure on head temperature were only accurate within about 15° to 20° F for exhaust pressures below approximately 10 and above approximately 50 inches of mercury absolute.

4. Calculations based on the test results indicated that for operation at constant power, equal to the engine normal rated power, at a fuel-air ratio of 0.085, the head temperature increased 39° F when the exhaust pressure was increased from 10 to 50 inches of mercury absolute. For operation at constant inlet-manifold pressure, however, the effect of mean effective gas temperature was for the most part counteracted by the effect of reduced power obtained with increased exhaust pressure; for example, for a constant inlet-manifold pressure of 30 inches of mercury absolute at a fuel-air ratio of 0.085 the head-temperature increase was only 7° F for an increase in exhaust pressure from 10 to 50 inches of mercury absolute.

5. The effect of exhaust pressure on engine cooling was greater at the lean than the rich mixtures.

Aircraft Engine Research Laboratory,
National Advisory Committee for Aeronautics,
Cleveland, Ohio, December 2, 1946.

APPENDIX A

SYMBOLS

The following symbols and abbreviations are used in the appendixes:

A	constant equal to engine mechanical friction horsepower divided by square of engine speed
bhp	engine brake horsepower
c_p	specific heat of air at constant pressure, 0.24 Btu/lb/°F
g	acceleration of gravity at standard conditions, 32.2 ft/sec ²
ihp	engine indicated horsepower
J	mechanical equivalent of heat, 778 ft-lb/Btu
K,m,n	constants derived from proper cooling data
k	ratio of supercharger pressure coefficient to adiabatic efficiency, assumed equal to 1
N	engine speed, rpm
p_e	exhaust pressure, in. Hg absolute
p_m	inlet-manifold pressure, in. Hg absolute
Δp	cooling-air pressure drop across engine, in. water
T_a	cooling-air temperature ahead of engine, °F
T_b	cylinder-barrel temperature, °F
T_c	charge-air temperature at carburetor inlet, °F
T_g	mean effective gas temperature, °F
$T_{g,80}$	mean effective gas temperature corrected to 80° F dry inlet-manifold temperature, °F
ΔT_g	change in mean effective gas temperature, °F

T_h	cylinder-head temperature, °F
T_m	dry inlet-manifold temperature, °F
U	tip speed of engine-stage supercharger, ft/sec
v_d	engine-displacement volume, cu ft
W_c	engine charge-air flow, lb/sec
W_f	total engine fuel consumption, lb/sec
η_g	efficiency of supercharger gears
σ	density of cooling air ahead of engine relative to standard sea-level density of 0.0765 lb/cu ft

APPENDIX B

CORRELATION OF COOLING DATA AT SEA-LEVEL EXHAUST PRESSURE

T_g relations. - The method used to evaluate T_g , which has been successfully applied to the correlation of numerous cooling data obtained for a large number of air-cooled engines, is outlined as follows:

1. On the basis of previous correlation work, a reference $T_{g,80}$ value of 1150° F for the heads and 600° F for the barrels was chosen for a fuel-air ratio of 0.080, a dry inlet-manifold temperature of 80° F, an exhaust pressure of 30 inches of mercury absolute, and the normal spark advance.

2. The variation of $T_{g,80}$ with fuel-air ratio is presented in figure 13 as determined from the cooling data obtained in a series of runs in which only the fuel-air ratio was varied. In this determination, the constant $\frac{T_h - T_a}{T_g - T_h}$ and $\frac{T_b - T_a}{T_g - T_b}$ values for the series (constant because of constancy of W_c and $\sigma \Delta p$) were calculated from the values of T_h , T_b , and T_a obtained in the run at a fuel-air ratio of 0.080 and the corresponding T_g values (1150° F for the heads and 600° F for the barrels plus the appropriate correction arising from the difference between the experimental and standard T_m values). Solution for T_g and hence for $T_{g,80}$ for the other fuel-air-ratio runs in the series was then made from the constant $\frac{T_h - T_a}{T_g - T_h}$ and $\frac{T_b - T_a}{T_g - T_b}$ values and the cooling measurements in each run.

3. The correction to $T_{g,80}$ applied for T_m values other than the standard value of 80° F is for the cylinder heads

$$\Delta T_g = 0.8 (T_m - 80) \quad (4)$$

and for the cylinder barrels

$$\Delta T_g = 0.5 (T_m - 80) \quad (5)$$

The dry inlet-manifold temperature T_m is calculated from the carburetor inlet-air temperature and the theoretical blower temperature rise assuming no fuel vaporization.

$$T_m = T_c + \frac{kU^2}{gJc_p} \quad (6)$$

This equation may be conveniently expressed for the engine used in this investigation as follows:

For low-blower ratio

$$T_m = T_c + 22.1 \left(\frac{N}{1000} \right)^2 \quad (7)$$

and for high-blower ratio

$$T_m = T_c + 34.2 \left(\frac{N}{1000} \right)^2 \quad (8)$$

Exponent on W_c . - The determination of the exponent n on charge-air flow W_c is shown in figure 14 where plots of $\frac{T_h - T_a}{T_g - T_h}$ and $\frac{T_b - T_a}{T_g - T_b}$ against W_c were made from the data obtained in a series of runs in which the fuel-air ratio was held constant at 0.080 and only the charge-air flow was varied. The T_g values used in the calculations correspond to a fuel-air ratio of 0.080 and the values of T_m . The exponent n on W_c is given by the slope of the line determined by the plotted points in figure 14 as 0.62 for the cylinder heads and 0.57 for the barrels.

Generalized correlation results. - The cooling-correlation results are presented in final form in figure 4 as plots of $\frac{T_h - T_a}{T_g - T_h} / W_c^{0.62}$ and $\frac{T_b - T_a}{T_g - T_b} / W_c^{0.57}$ against cooling-air pressure drop $\sigma\Delta p$. The cooling data obtained from all the sea-level exhaust-pressure runs are included in these plots. The cooling-correlation equation representing the correlation line through the plotted values in figure 4 is expressed as follows:

For the cylinder heads

$$\frac{T_h - T_a}{T_g - T_h} = 0.44 \frac{W_c^{0.62}}{(\sigma\Delta p)^{0.30}} \quad (2)$$

and for the cylinder barrels

$$\frac{T_b - T_a}{T_g - T_b} = 0.68 \frac{W_c^{0.57}}{(\sigma\Delta p)^{0.39}} \quad (3)$$

APPENDIX C

ESTIMATION OF CHARGE-AIR FLOW

Charge-air flow is the fundamental variable in engine cooling, whereas engine performance is usually specified in terms of brake horsepower, speed, fuel-air ratio, and inlet-manifold and exhaust pressures. It is therefore essential prior to the application of the cooling-correlation results, to estimate the charge-air flow from the known engine-performance variables. This estimate can be obtained from the relation between the charge air pumped and the indicated horsepower developed by an engine. The assumption involved in this relation, which has been satisfactorily verified for current engines and operating ranges, is that the charge-air flow per indicated engine horsepower is primarily a function of fuel-air ratio.

As presented in reference 4, the indicated horsepower developed by an engine is related to the known engine operating conditions by the general expression

$$\text{ihp} = \text{bhp} + k \left(\frac{U}{N} \right)^2 \frac{(W_c + W_f) N^2}{550 g \eta_g} + v_d (p_e - p_m) \frac{N}{933} + AN^2 \quad (9)$$

where

AN^2 mechanical friction horsepower

$k \left(\frac{U}{N} \right)^2 \frac{(W_c + W_f) N^2}{550 g \eta_g}$ supercharging horsepower

$v_d (p_e - p_m) \frac{N}{933}$ pumping horsepower (intake and exhaust strokes)

The constant A in the friction-horsepower term was determined as 32.1 from an empirical relation based on data from a large number of similar engines. As in reference 5, the factors k and η_g in the supercharging-horsepower term are equal to 1 and 0.85, respectively. The value of U/N is obtained from the supercharger-impeller diameter and gear ratio.

The general expression for indicated horsepower can thus be reduced for the engine used in the subject tests to the following equations:

Low-blower ratio

$$ihp = bhp + \left[32.1 + 8.84 (W_c + W_f) \right] \left(\frac{N}{1000} \right)^2 - 1.74 (p_m - p_e) \frac{N}{1000} \quad (10)$$

High-blower ratio

$$ihp = bhp + \left[32.1 + 13.67 (W_c + W_f) \right] \left(\frac{N}{1000} \right)^2 - 1.74 (p_m - p_e) \frac{N}{1000} \quad (11)$$

The good correlation of engine-performance data resulting from the use of the charge-air flow indicated-horsepower relation is illustrated in figure 15 for typical test conditions covering the engine operating range of the investigation. The validity and accuracy of this relation is more conclusively confirmed in reference 3 from a consideration of all the performance data obtained.

Inasmuch as, for the usual engine application, the brake horsepower is not held constant when the exhaust pressure is changed but is permitted to vary in the manner obtained by maintaining constant inlet-manifold pressure, the relation describing the variation of brake horsepower with exhaust pressure for constant inlet-manifold pressure and other constant engine operating conditions is also required for use with equations (10) and (11) and figure 15 to determine the variation in charge-air flow with exhaust pressure. This relation was determined in reference 3 from all the performance data obtained in the tests and, for convenience of application to the cooling-correlation results, is presented in figure 16. The ratio of the engine brake horsepower developed at a given value of p_e/p_m to that developed at $p_e/p_m = 1$ for constant fuel-air ratio, inlet-manifold pressure and temperature, engine speed, and engine-stage supercharger gear ratio is presented for the test range of engine speeds (fig. 16). These curves were found to be applicable for the test range of fuel-air ratios, inlet-manifold pressures, and for both high- and low-supercharger gear ratio.

If the change in exhaust pressure is caused by a change in altitude, then, in addition to the T_g correction given by figure 8, a correction must be made for the change in charge-air temperature at the inlet manifold.

REFERENCES

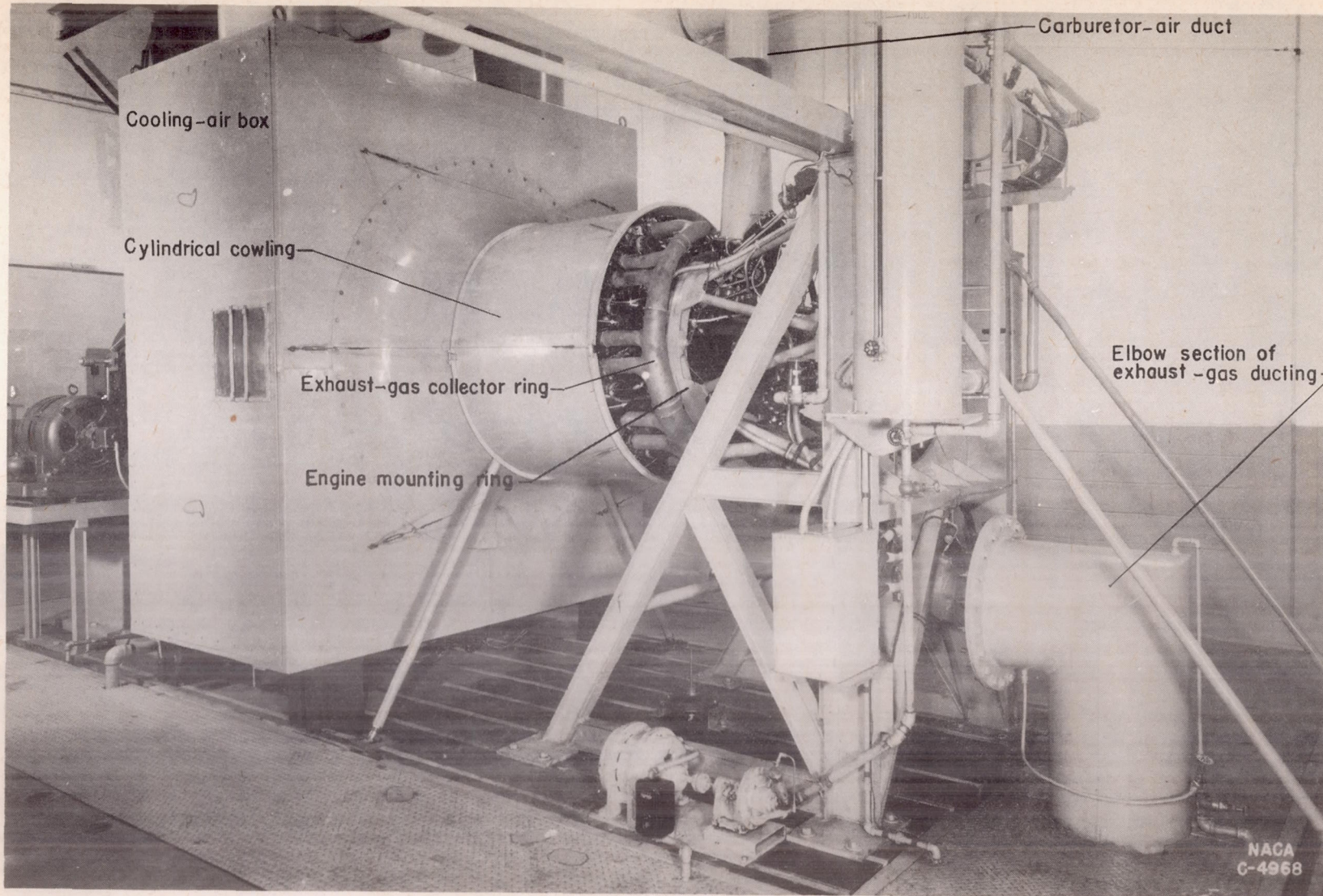
1. Pinkel, Benjamin: Heat-Transfer Processes in Air-Cooled Engine Cylinders. NACA Rep. No. 612, 1938.
2. Pinkel, Benjamin, and Ellerbrock, Herman H., Jr.: Correlation of Cooling Data from an Air-Cooled Cylinder and Several Multi-cylinder Engines. NACA Rep. No. 683, 1940.
3. Boman, David S., Nagey, Tibor F., and Doyle, Ronald B.: Effect of Exhaust Pressure on the Performance of an 18-Cylinder Air-Cooled Radial Engine with a Valve Overlap of 40° . NACA TN No. , 1946.
4. Pinkel, Benjamin, and Rubert, Kennedy F.: Correlation of Wright Aeronautical Corporation Cooling Data on the R-3350-14 Intermediate Engine and Comparison with Data from the Langley 16-Foot High-Speed Tunnel. NACA ACR No. E5A18, 1945.
5. Corson, Blake W., Jr., and McLellan, Charles H.: Cooling Characteristics of a Pratt & Whitney R-2800 Engine Installed in a NACA Short-Nose High-Inlet-Velocity Cowling. NACA ACR No. L4FC6, 1944.

TABLE I - OPERATING CONDITIONS
 [Carburetor-air temperature, $90^{\circ} \pm 15^{\circ}$ F]

Normal engine speed (rpm)	Nominal fuel-air ratio	Nominal inlet- manifold pressure (in. Hg absolute)
Sea-level exhaust-pressure test group (basic correlation)		
Varied	0.085	34
2000	.085	Varied
2000	Varied	30
Variable exhaust-pressure test group (a)		
1200, 1400, 1600, 1800, 2000	0.069	30
1400, 1600, 1800, 2000, 2200, 2400	.085	30
2000, 2200, 2400	.100	30
1400, 1600, 1800, 2000	.069	34
1400, 1600, 1800, 2000, 2200, 2400	.085	34
2000, 2200	.100	34
1400, 1600, 1800, 2000	.069	40
1600, 1800, 2000, 2200, 2400	.085	40
1800, 2000, 2200, 2400	.100	40
1800, 2000, 2200	.085	45
1800, 2000, 2200, 2400	.100	45
1800, 2000	.120	40

^aThe exhaust pressure for this group was varied in steps from approximately 7 inches of mercury absolute to 20 inches of mercury above inlet-manifold pressure.

National Advisory Committee
 for Aeronautics



NACA TN No. 1221

Fig. 1

Figure 1. - General view of installation of 18-cylinder, radial, air-cooled engine.

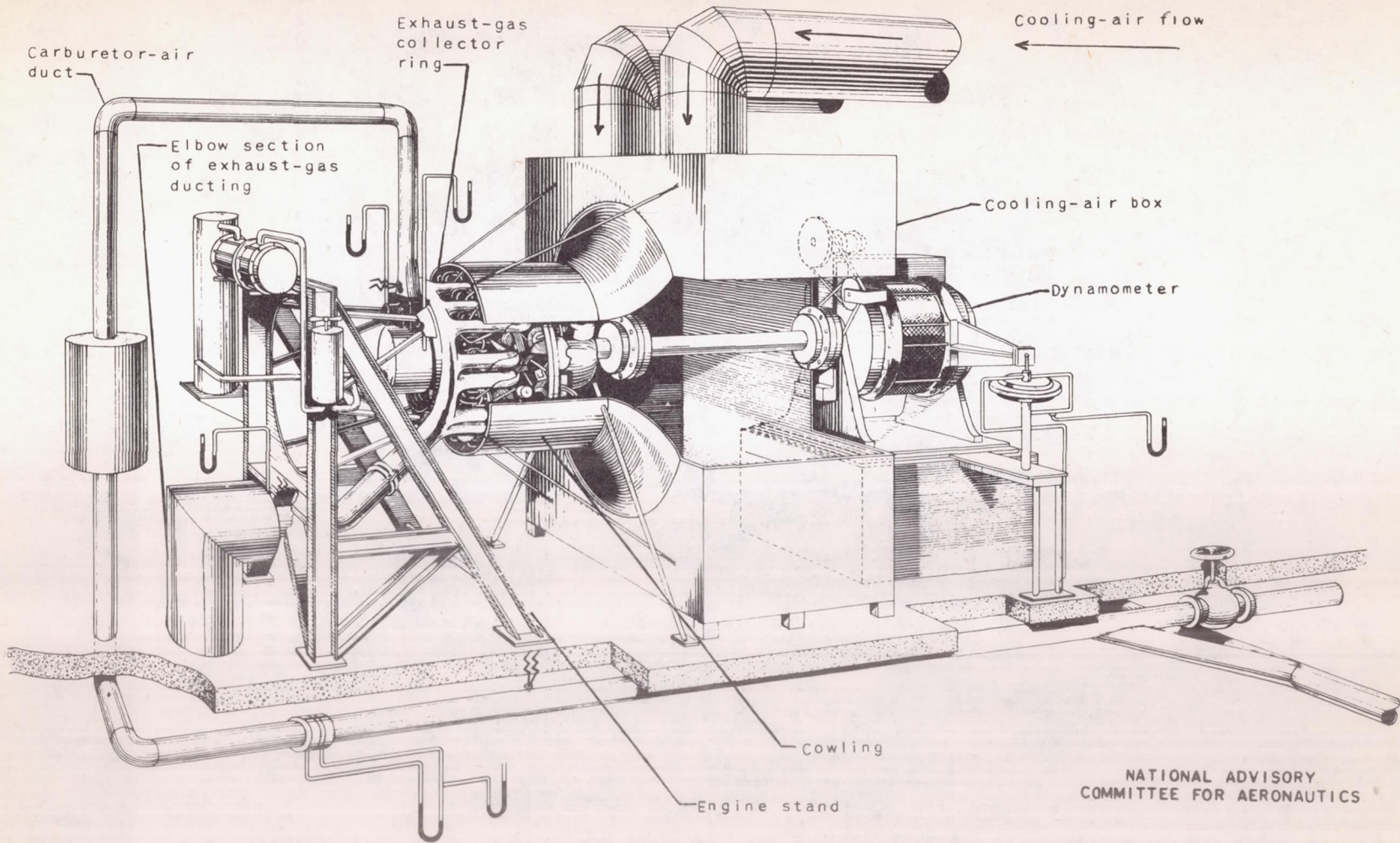


Figure 2. - Diagrammatic sketch of installation of 18-cylinder, radial, air-cooled engine.

NATIONAL ADVISORY COMMITTEE FOR AERONAUTICS

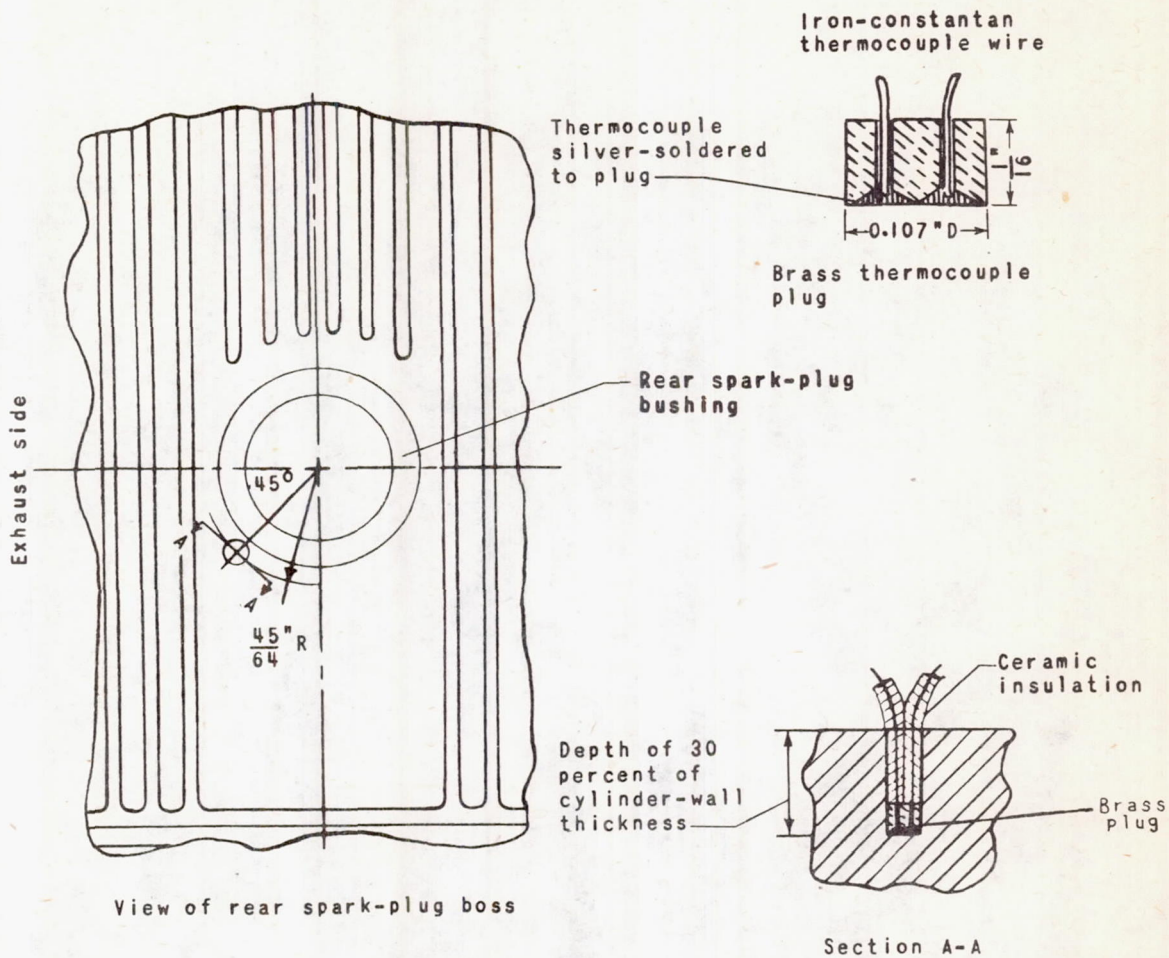


Figure 3. - Standard NACA deep-embedded rear-spark-plug-boss thermocouple installation.

NATIONAL ADVISORY
COMMITTEE FOR AERONAUTICS

NATIONAL ADVISORY
COMMITTEE FOR AERONAUTICS

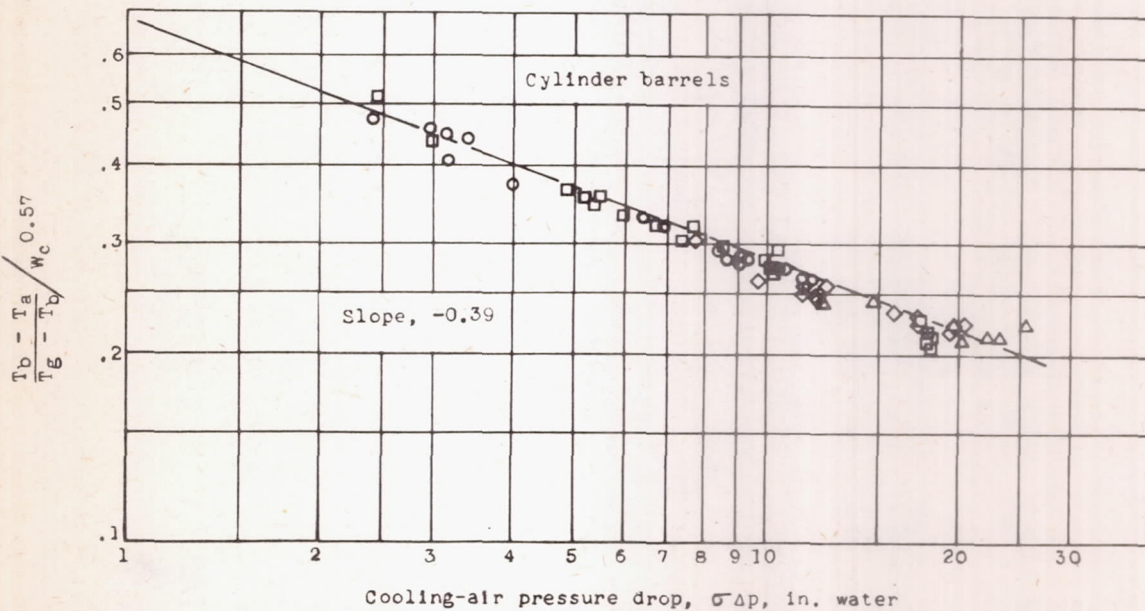
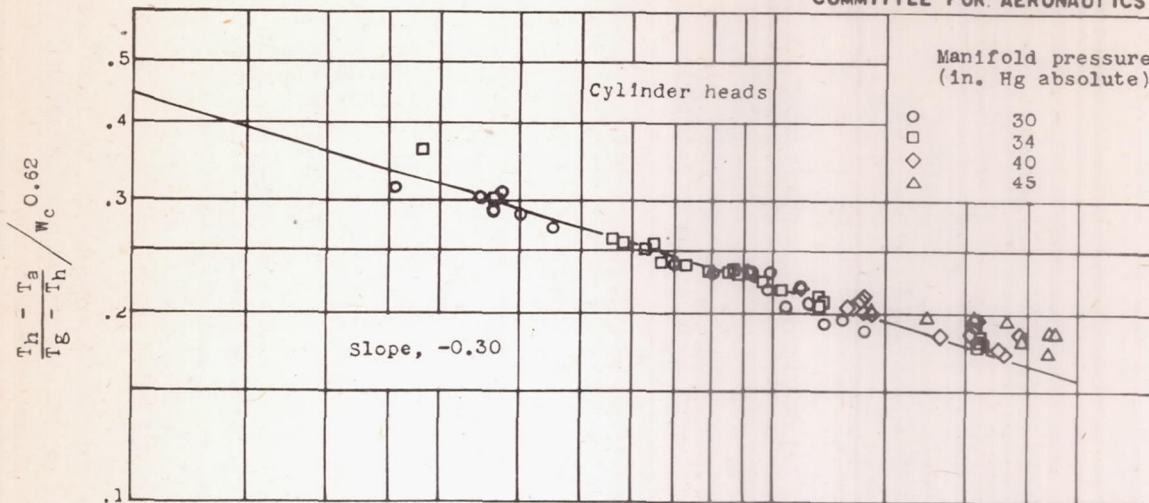
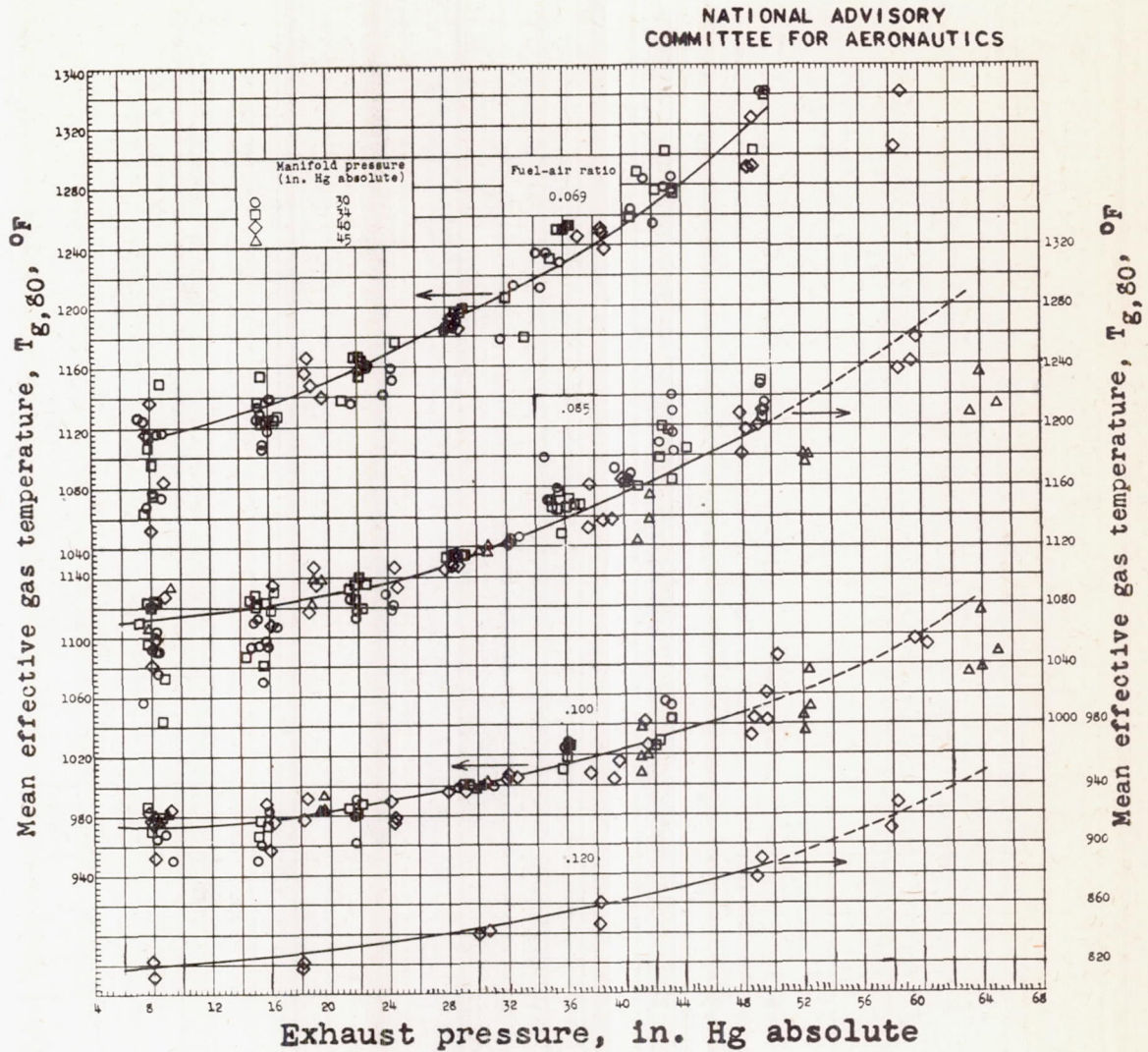
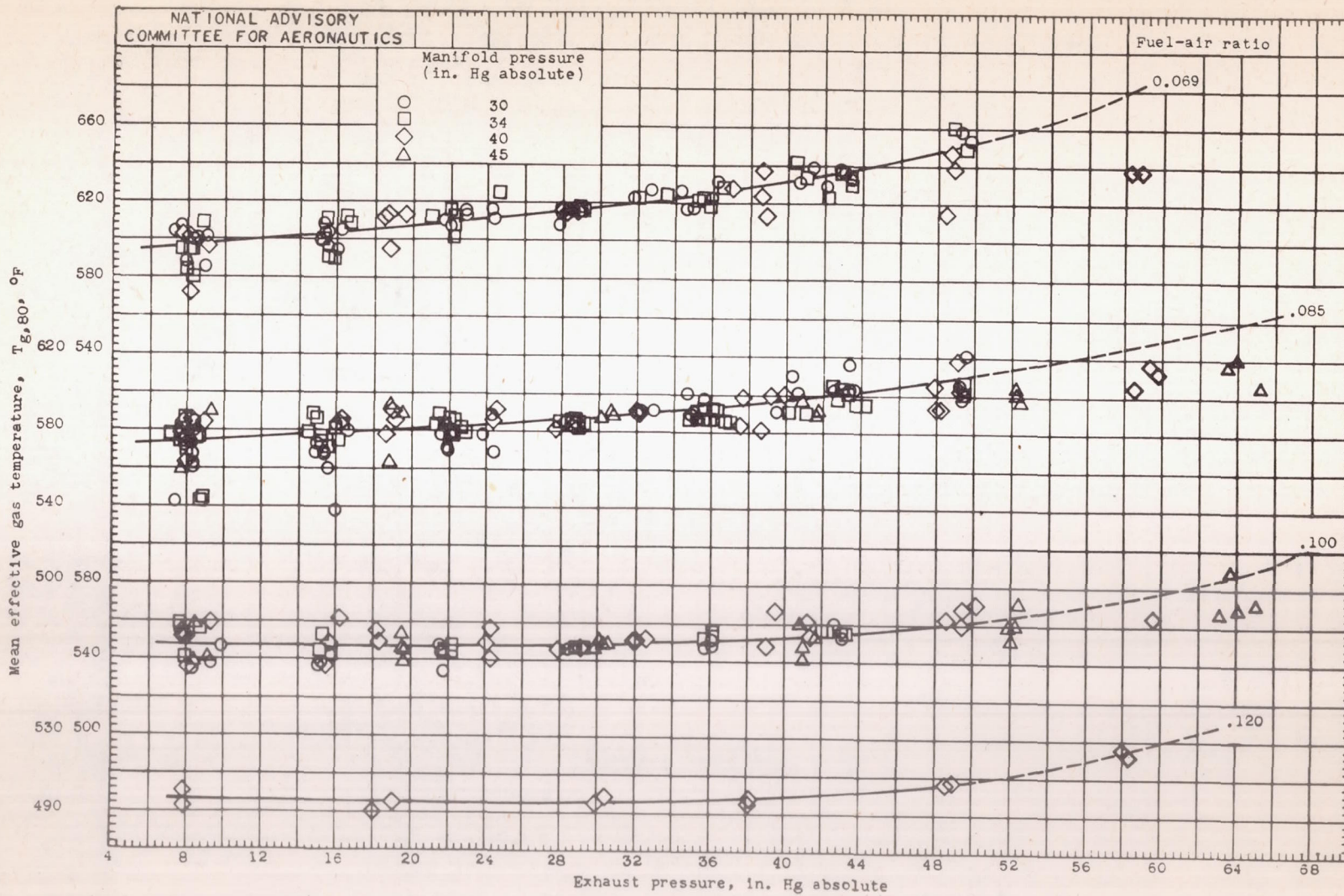


Figure 4. - Cooling correlation for an 18-cylinder, radial, air-cooled engine. Exhaust pressure, approximately 30 inches mercury absolute; fuel-air ratio, 0.069 to 0.120; engine speed, 1200 to 2400 rpm.



(a) Cylinder heads.

Figure 5. - Effect of exhaust pressure on the mean effective gas temperature at various fuel-air ratios for an 18-cylinder, radial, air-cooled engine.



(b) Cylinder barrels.

Figure 5. - Concluded. Effect of exhaust pressure on the mean effective gas temperature at various fuel-air ratios for an 18-cylinder, radial, air-cooled engine.

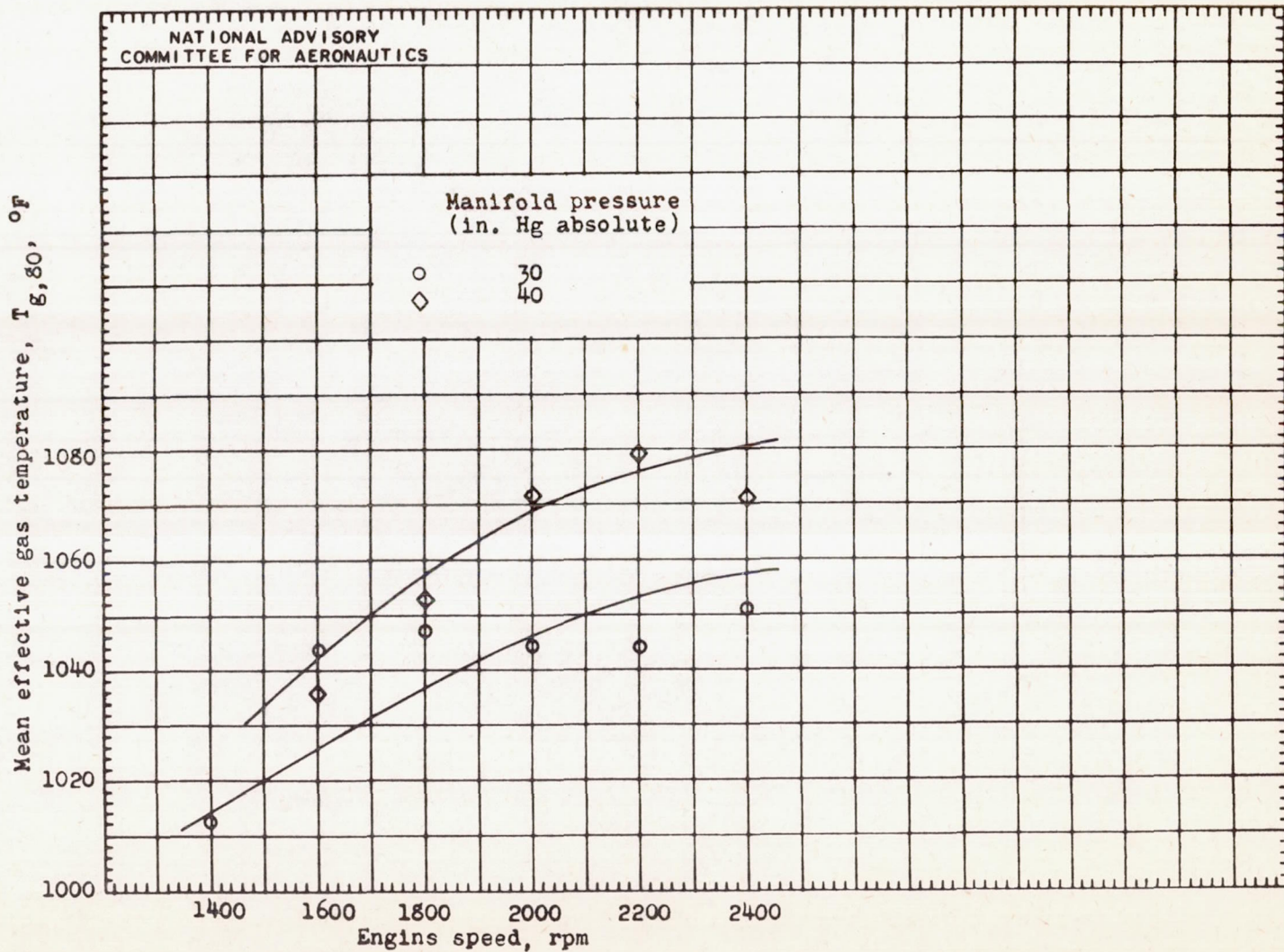


Figure 6. - Variation of mean effective gas temperature for cylinder heads with engine speed at low exhaust pressure for an 18-cylinder, radial, air-cooled engine. Exhaust pressure, approximately 8 inches mercury absolute; fuel-air ratio, 0.085.

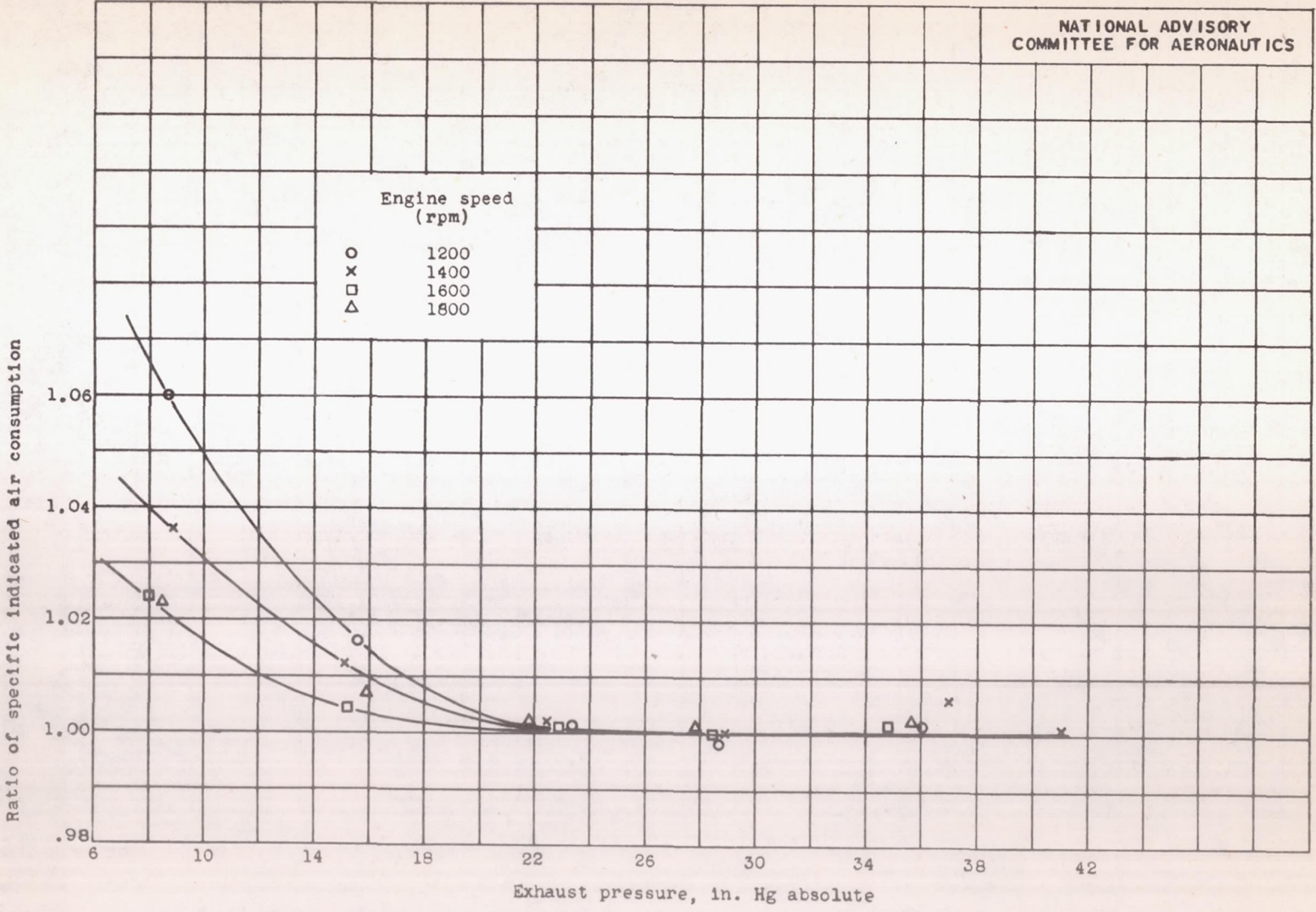


Figure 7. - Ratio of specific indicated air consumption obtained at various exhaust pressures to the specific indicated air consumption obtained at $p_e/p_m = 1$ from tests of an 18-cylinder, radial, air-cooled engine. Fuel-air ratio, 0.085; manifold pressure, 34 inches mercury absolute.

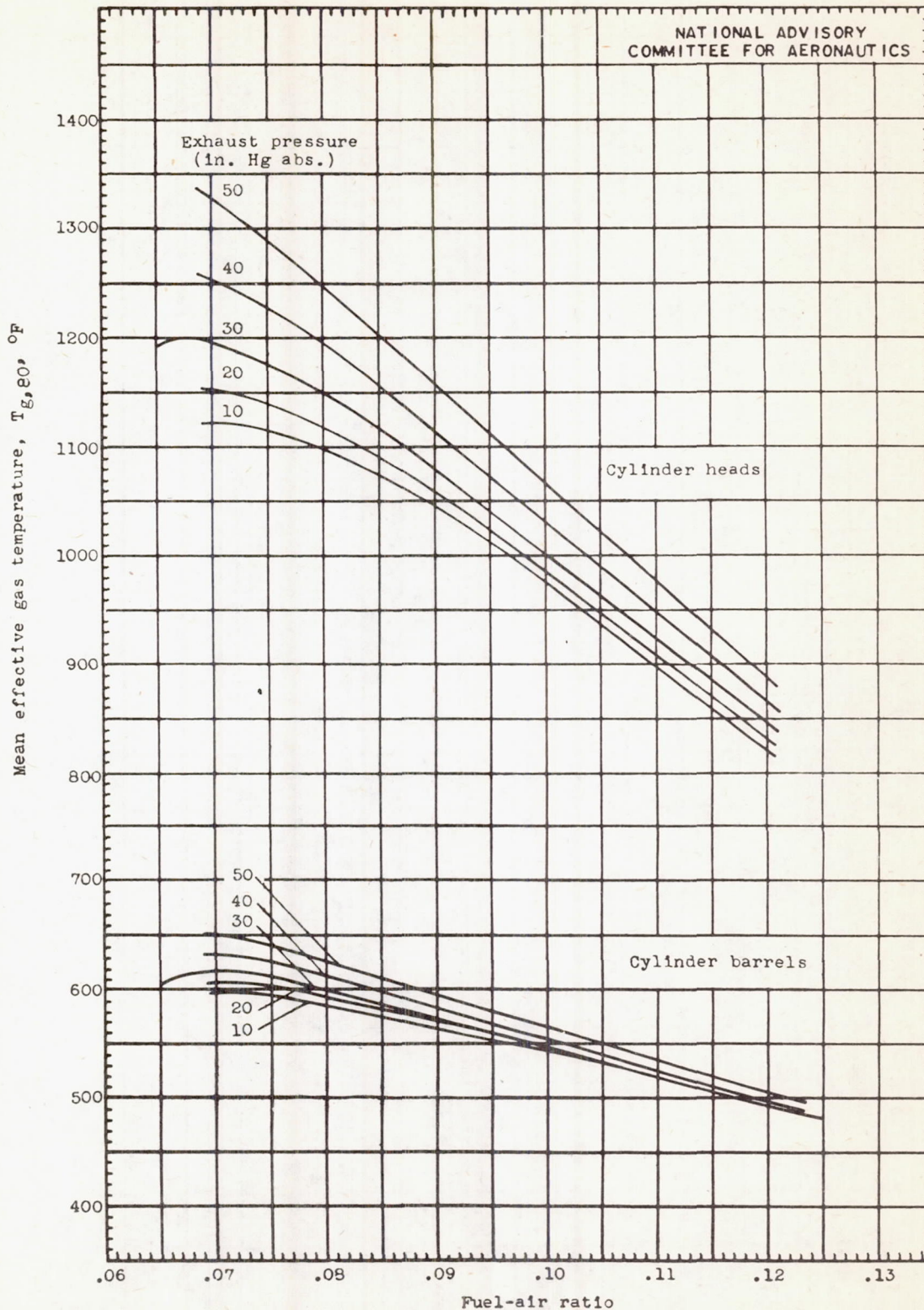
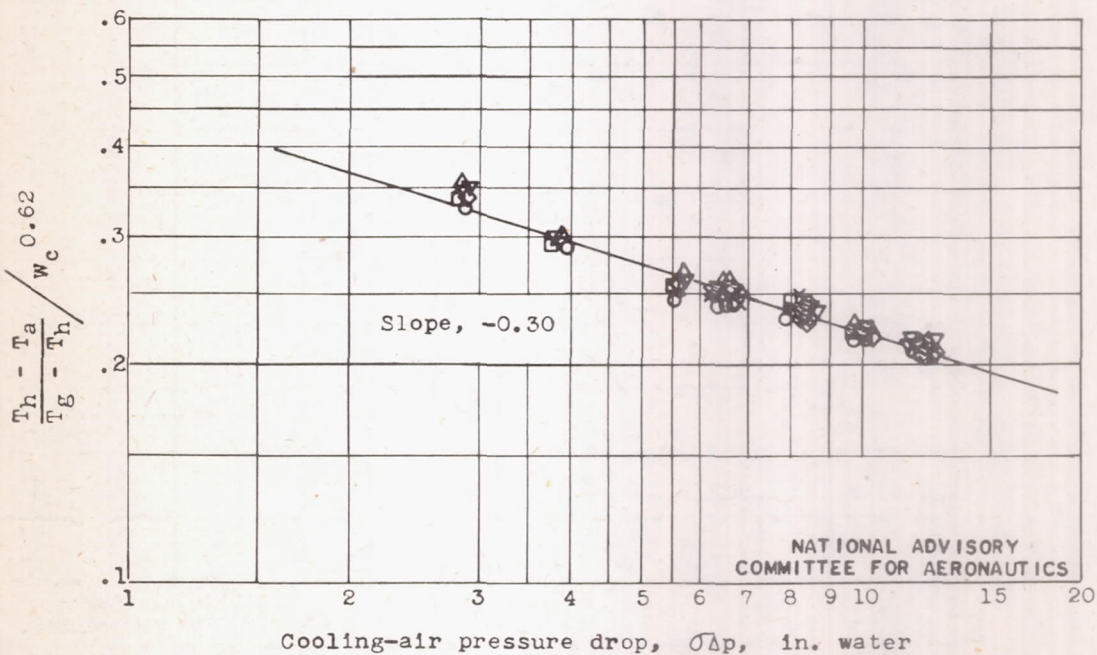
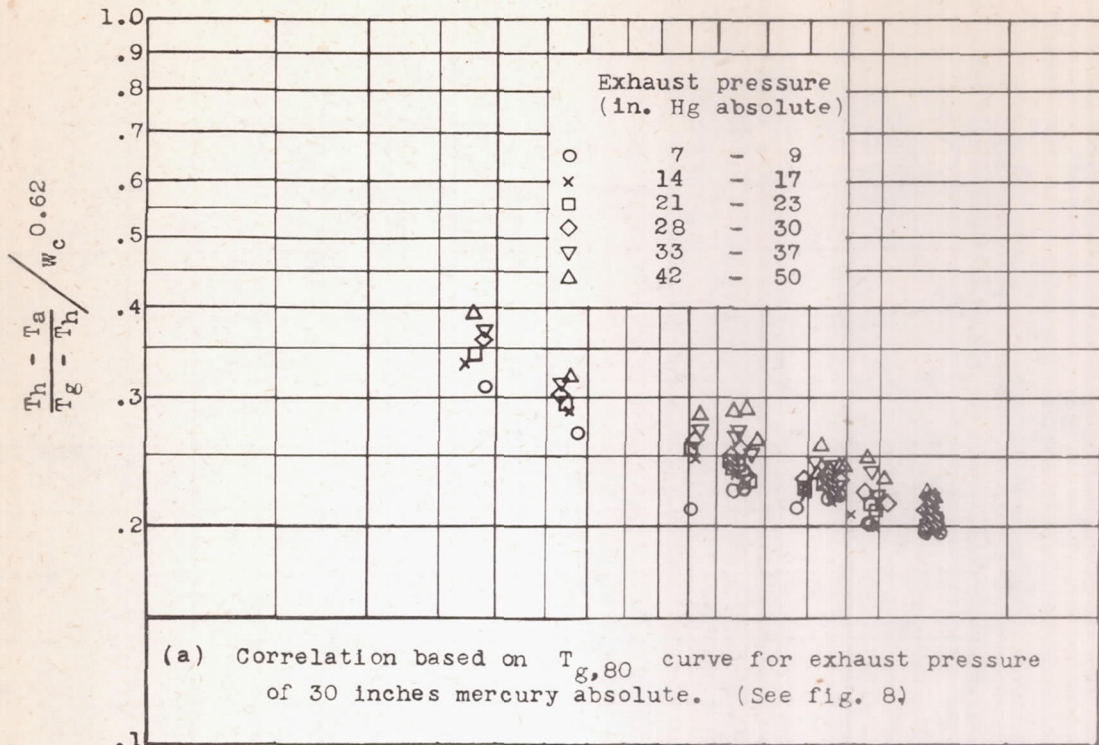


Figure 8. - Variation of mean effective gas temperature with fuel-air ratio at various exhaust pressures for cylinder heads and barrels of an 18-cylinder, radial, air-cooled engine. (Cross plot of fig. 5)



(b) Correlation based on $T_{g,80}$ curve corrected for exhaust pressure. (See fig. 8)

Figure 9. - Cooling-correlation curve for an 18-cylinder, radial, air-cooled engine. Cylinder-head cooling data obtained at a manifold pressure of 34 inches mercury absolute and at variable exhaust pressure.

687

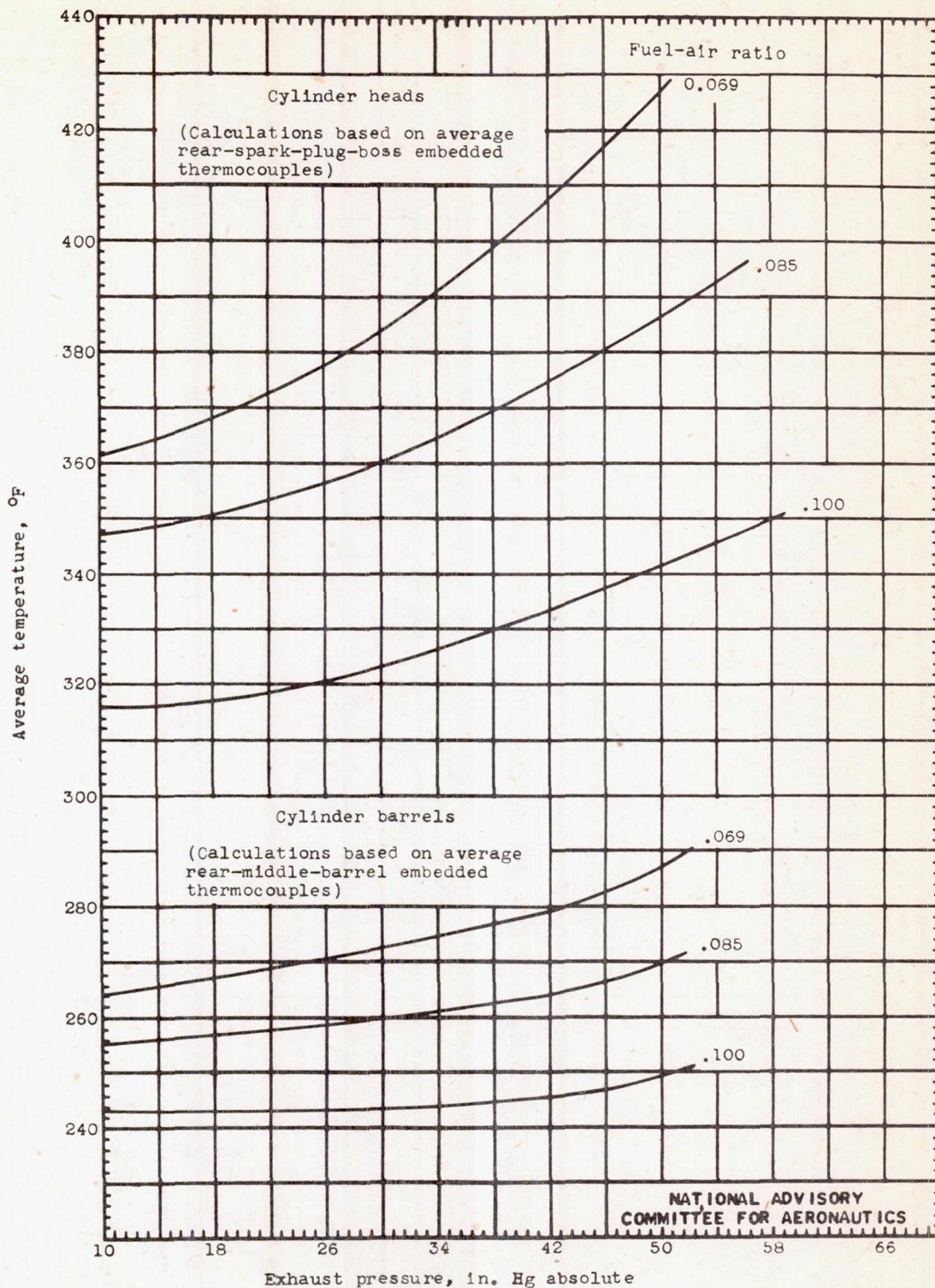


Figure 10. - Variation of average head and barrel temperatures with exhaust pressure for constant charge-air flow for an 18-cylinder, radial, air-cooled engine. Assumed conditions: charge-air flow, 3.0 pounds per second; manifold temperature, 150° F; cooling-air temperature, 0° F; cooling-air pressure drop maintained constant.

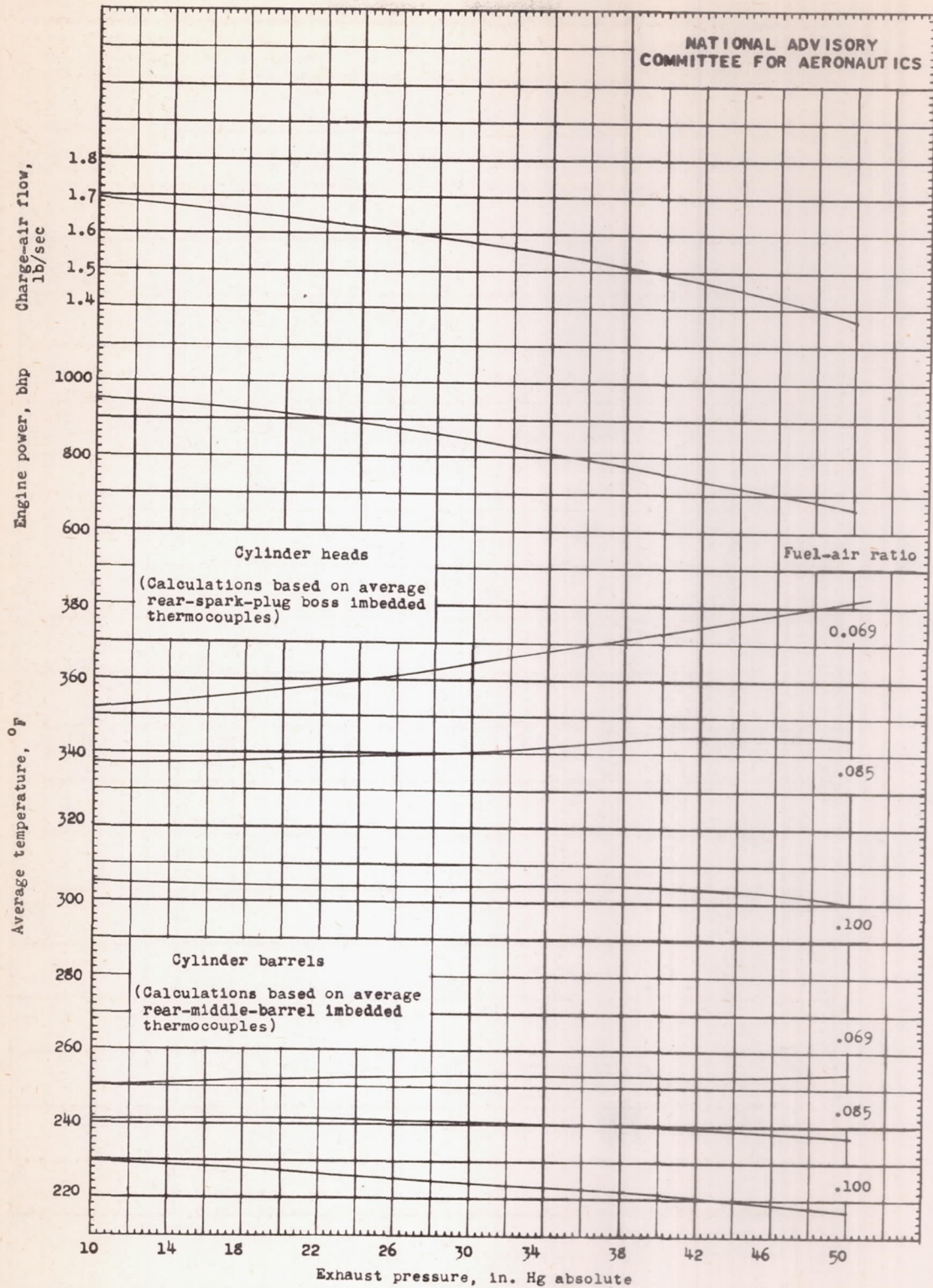


Figure 11. - Variation of average head and barrel temperatures with exhaust pressure for constant inlet-manifold pressure for an 18-cylinder, radial, air-cooled engine. Manifold pressure, 30 inches mercury absolute; engine speed, 2000 rpm; manifold temperature, 150° F; cooling-air temperature, 0° F; cooling-air pressure drop maintained constant.

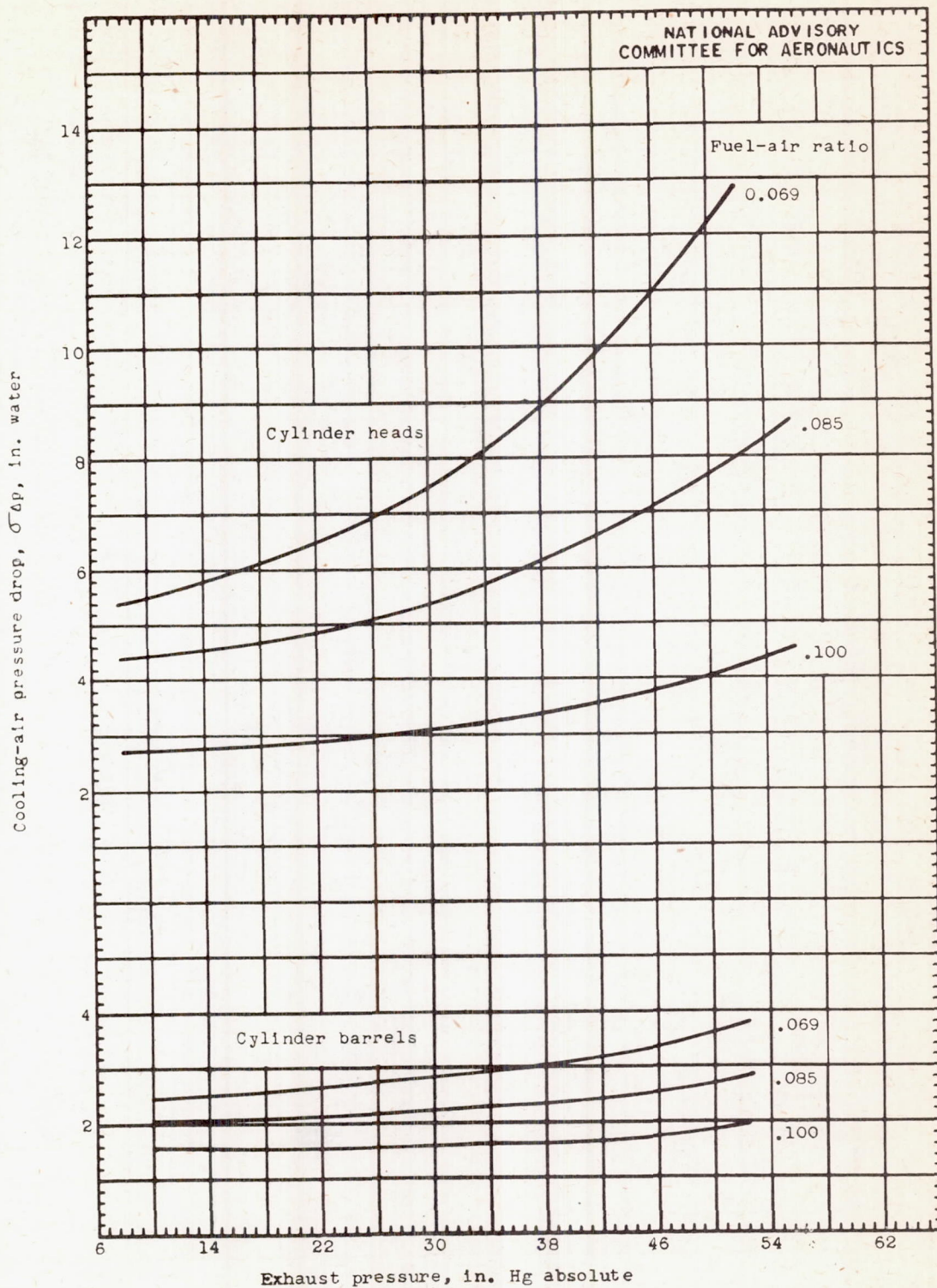


Figure 12. - Variation of cooling-air pressure drop with exhaust pressure for cylinder head and barrels for constant charge-air flow for an 18-cylinder, radial, air-cooled engine. Charge-air flow, 3.0 pounds per second; manifold temperature, 150° F; average head temperature, 400° F; average barrel temperature, 300° F; cooling-air temperature, 0° F.

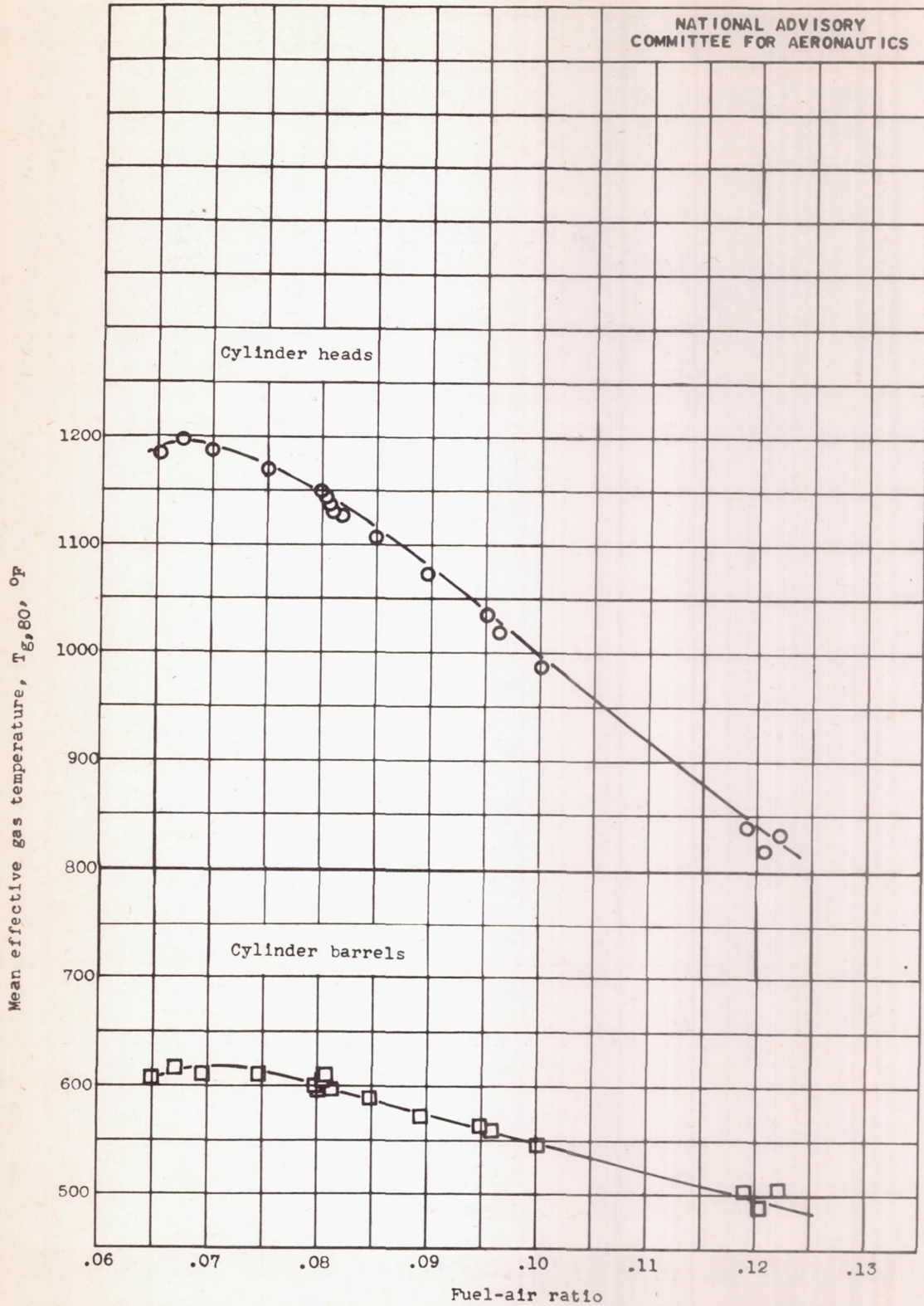


Figure 13. - Variation of mean effective gas temperature with fuel-air ratio for cylinder heads and barrels for an 18-cylinder, radial, air-cooled engine. Exhaust pressure, 30 inches mercury absolute.

687

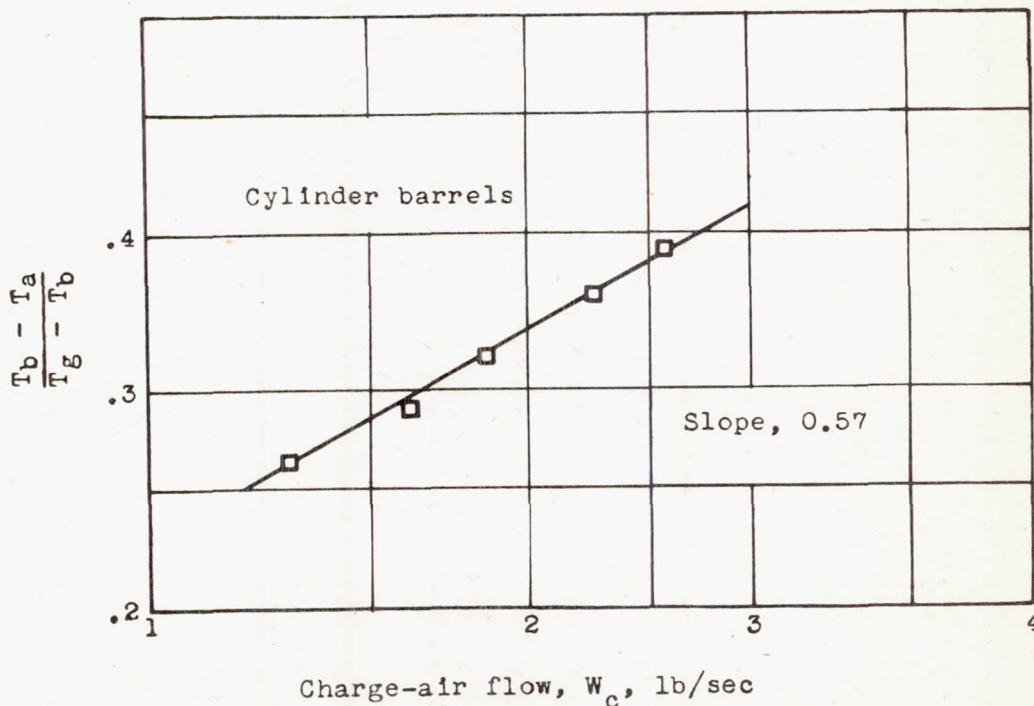
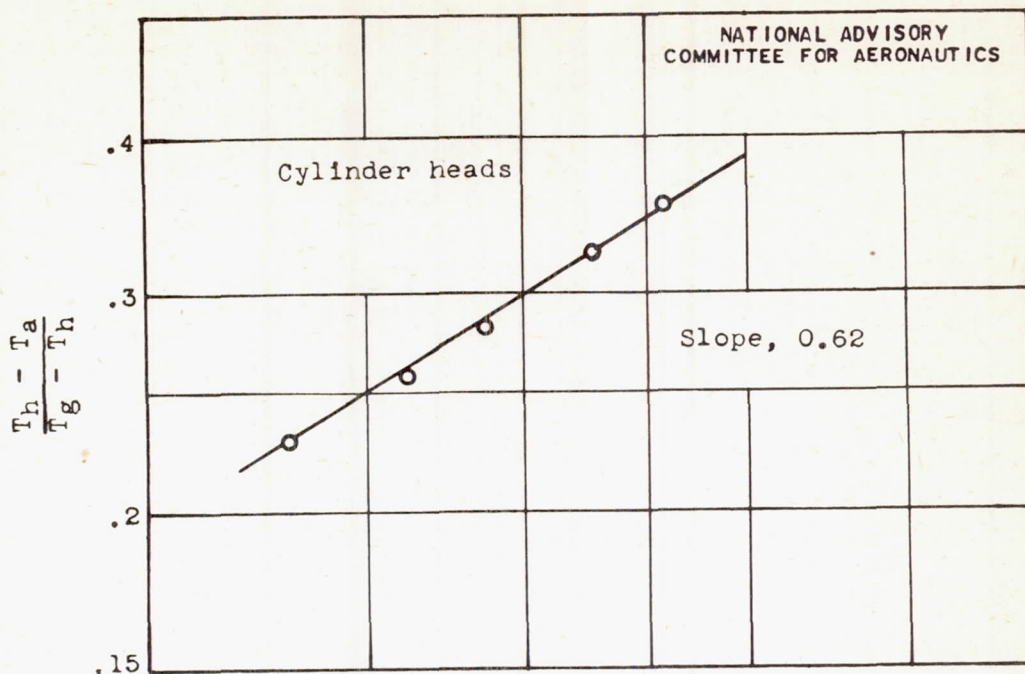


Figure 14. - Variation of $\frac{T_h - T_a}{T_g - T_h}$ and $\frac{T_b - T_a}{T_g - T_b}$ with charge-air

flow for an 18-cylinder, radial, air-cooled engine for constant cooling-air pressure drop. Fuel-air ratio, 0.080; exhaust pressure, 30 inches mercury absolute.

687

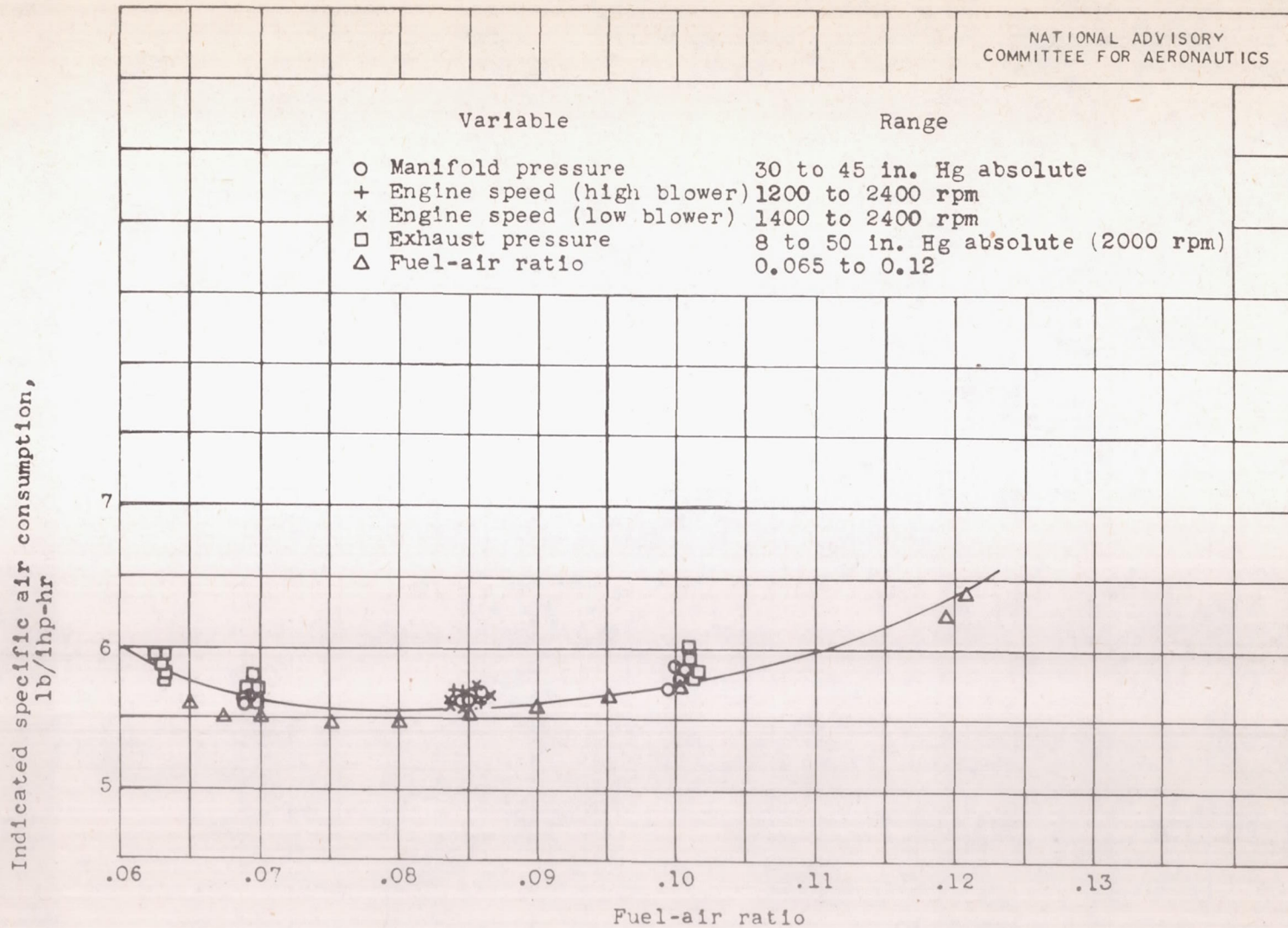


Figure 15. - Variation of specific indicated air consumption with fuel-air ratio for an 18-cylinder, radial, air-cooled engine.

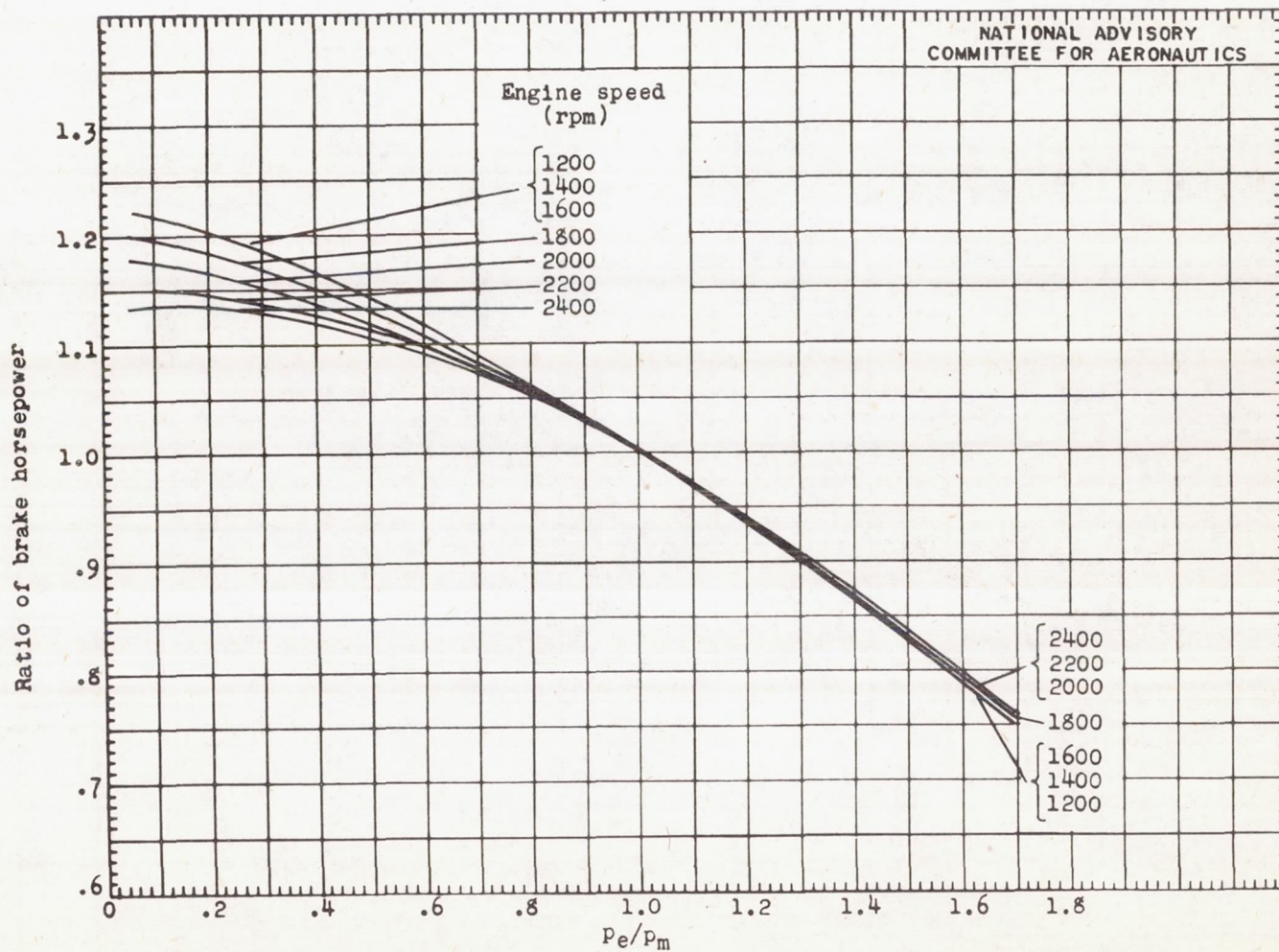


Figure 16. - Ratio of brake horsepower at any p_e/p_m to brake horsepower at $p_e/p_m = 1$ for various constant engine speeds for an 18-cylinder, radial, air-cooled engine. Fuel-air ratio, manifold pressure and temperature, and engine-stage supercharger gear ratio constant. (Reproduced from reference 3.)